Supporting Information

A Ni^{II} Complex of Tetradentate Salen Ligand $H_2L^{NH_2}$ Comprising an Anchoring $–NH_2$ Group: Synthesis, Characterization and Electrocatalytic CO_2 Reduction to Alcohols

Paulomi Bose[a], Chandan Mukherjee [a,b,*] and Animes Kumar Golder [a,c]

[a] Centre for the Environment, Indian Institute of Technology Guwahati, Assam-781039, INDIA [b] Department of Chemistry, Indian Institute of Technology Guwahati, Assam-781039, INDIA. Email: cmukherjee@iitg.ac.in., Phone: +91-361-2582327, Fax + 91-361-2582349. [c] Department of Chemical Engineering, Indian Institute of Technology Guwahati, Assam-781039, INDIA.

Contents	Page

Table S1: Comparison of the formation of ERC products and FE using various electrocatalysts in ERC.

Catalysts	**Reduction potential**	**Electrolyte**	**Products (%, FE)**	**References**
Ni metal	E_{cat} = − 1.84 V vs. Ag/AgCl	0.05 M $KHCO_3$	CO (21.0), HCOOH (13.7)	(1)
Nitrogen-doped nanodiamond	E_{cat} = −1.67 V vs. Ag/AgCl	0.5 M $NaHCO_3$	Acetate and Formate (90)	(2)
Au foil catalysts	E_{cat} = -1.35 V vs. Ag/AgCl	0.1 M $KHCO_3$	CO (97)	(3)
di-nuclear nickel complex	E_{cat} = -1.16 V vs. NHE	4 : 1 CH_3CN/H_2O	CO (95)	(4)
$M^{n+}(cyclam)Cl_n]$ (M = Ni^{2+})	E_{cat} = -1.4 V vs. Ag/AgCl	$BMImBF_4$ and $BMImNTf_2$	CO (95.2)	(5)
$M^{n+}(cyclam)Cl_n]$ (M = Co^{2+})	E_{cat} = -1.4 V vs. Ag/AgCl	$BMImBF_4$ and $BMImNTf_2$	CO (85.9)	(5)
Molecular polypyridyl nickel complex	E_{cat} = -1.86 V vs. Ag/AgCl	MeCN solution with 0.1 M $TBAPF_6$	CO (91)	(6)
Salen Ni- complex	E_{cat} = -1.80 V vs. Ag/AgCl	0.5 M $KHCO_3$	HCOOH (4.7), CH_3OH (11.4), C_2H_5OH (28.6)	**Present study**

Table S2: Calculated TON and TOF of the formation of ERC products using Ni Complex **1** in our study.

Product	V vs. Ag/AgCl	TOF (S^{-1})	TON
C_2H_5OH	-1.8	2.1	7560
HCOOH	-1.8	0.33	1214
CH_3CHO	-1.8	0.3	1270
CH_3OH	-1.8	0.8	3060

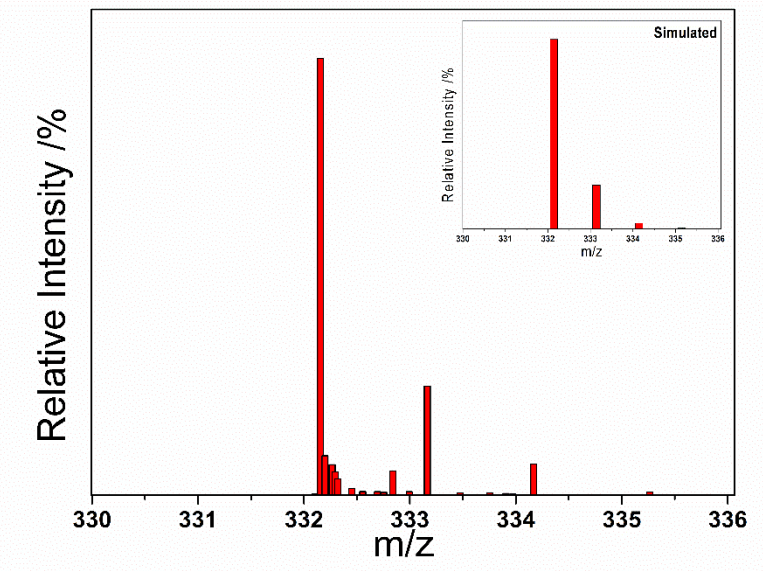

Figure S1: Experimental and simulated mass spectrum of synthesized ligand $\mathbf{H_2L^{NH}_2}$ [$C_{20}H_{17}N_3O_2$ + H].

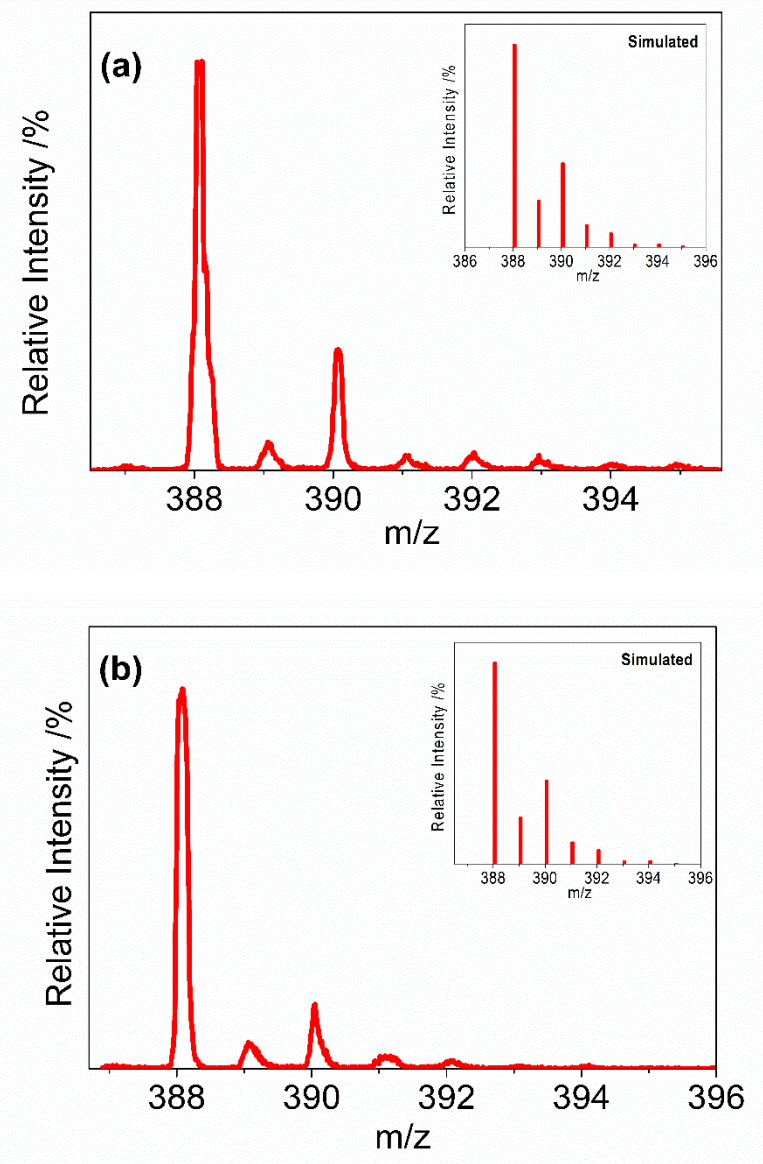

Figure S2: Experimental and simulated mass spectrum of complex **1** [$C_{20}H_{15}N_3O_2Ni$ + H] before (a) and after the ERC reaction (b).

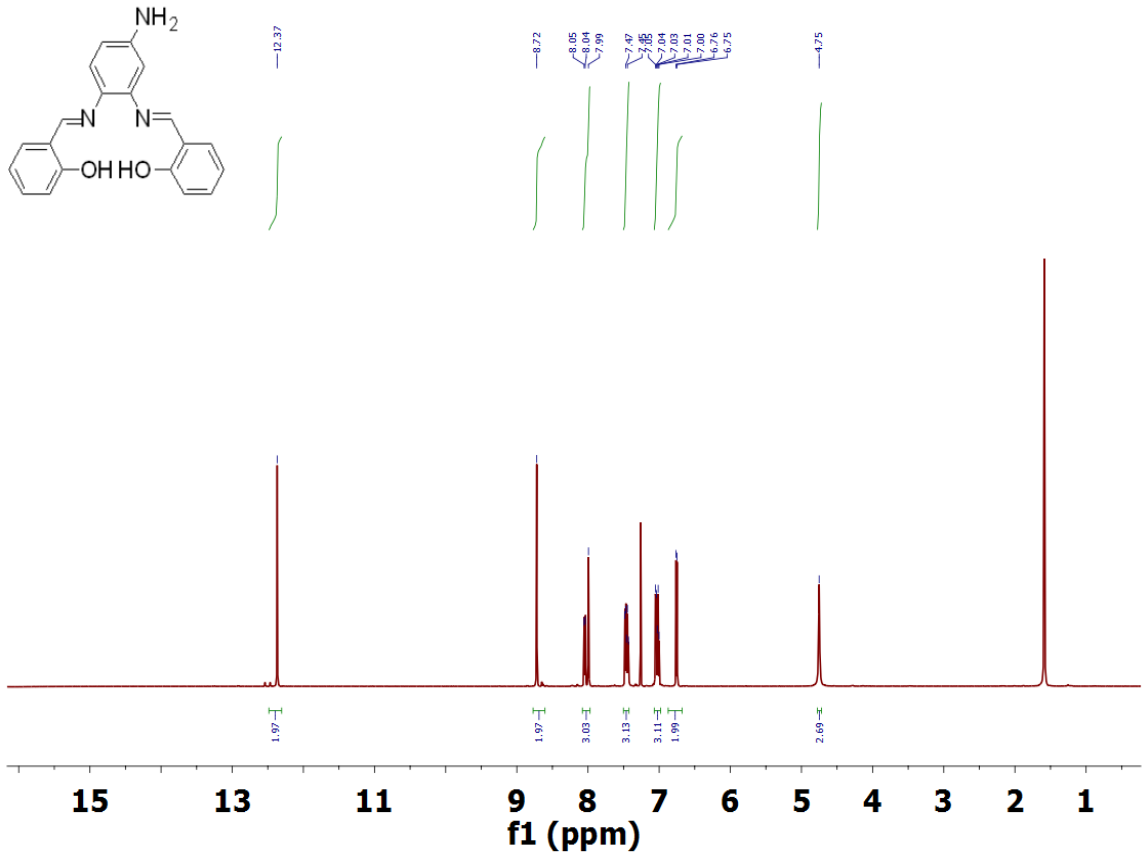

Figure S3: ^{1}H NMR spectrum of synthesized ligand $\mathbf{H_2L^{NH}_2}$ (in $CDCl_3$).

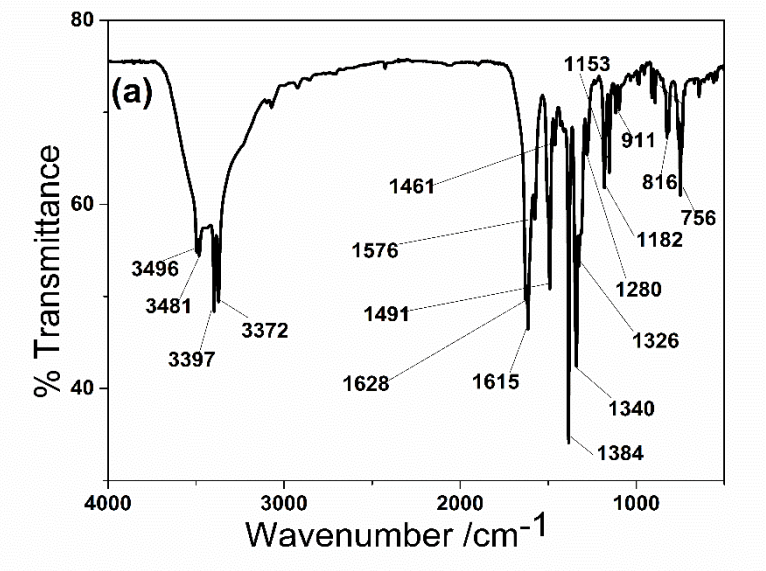

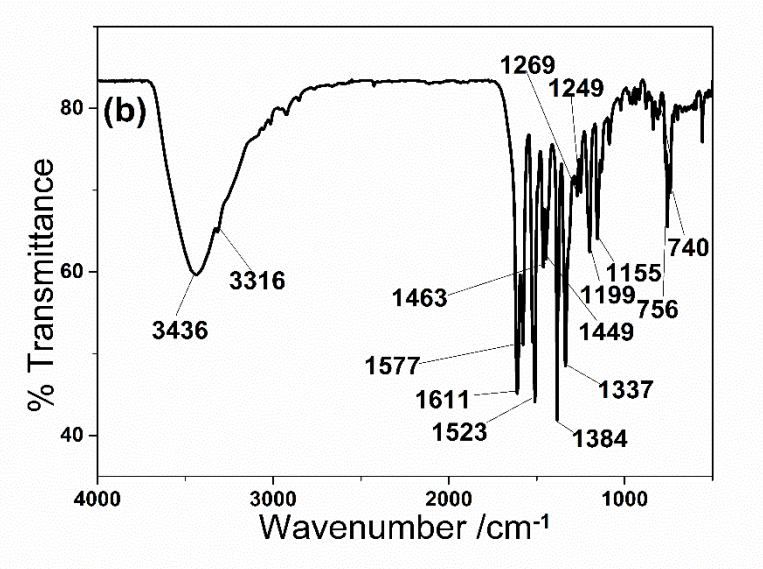

Figure S4: FTIR spectrum of (a) ligand $\mathbf{H_2L^{NH_2}}$ and (b) corresponding Ni complex (**1**).

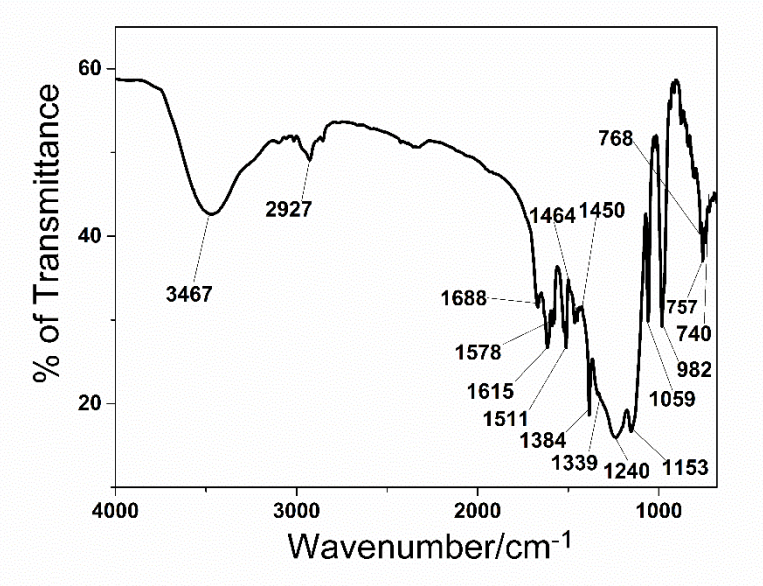

Figure S5: FTIR spectrum of electrode material after ERC reaction.

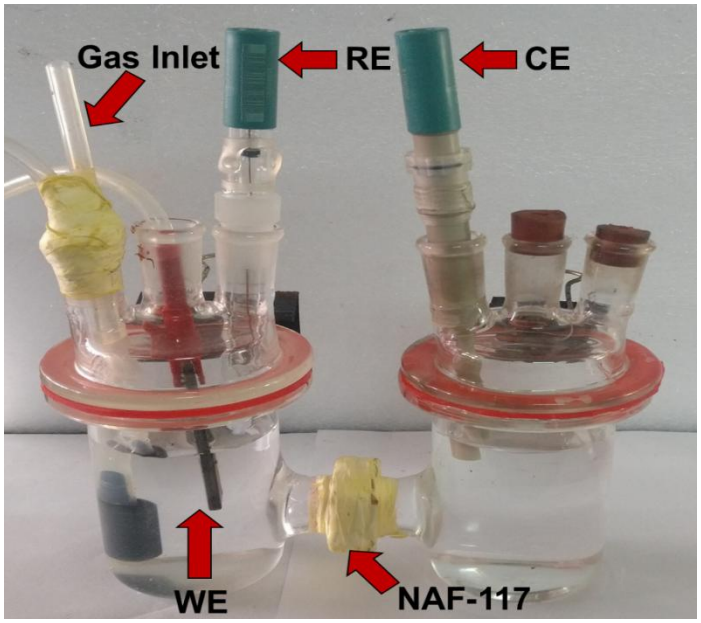

Figure S6: Digital image of the custom made H type divided electrochemical cell, WE= Working electrode, CE = Counter electrode, and RE= reference electrode.

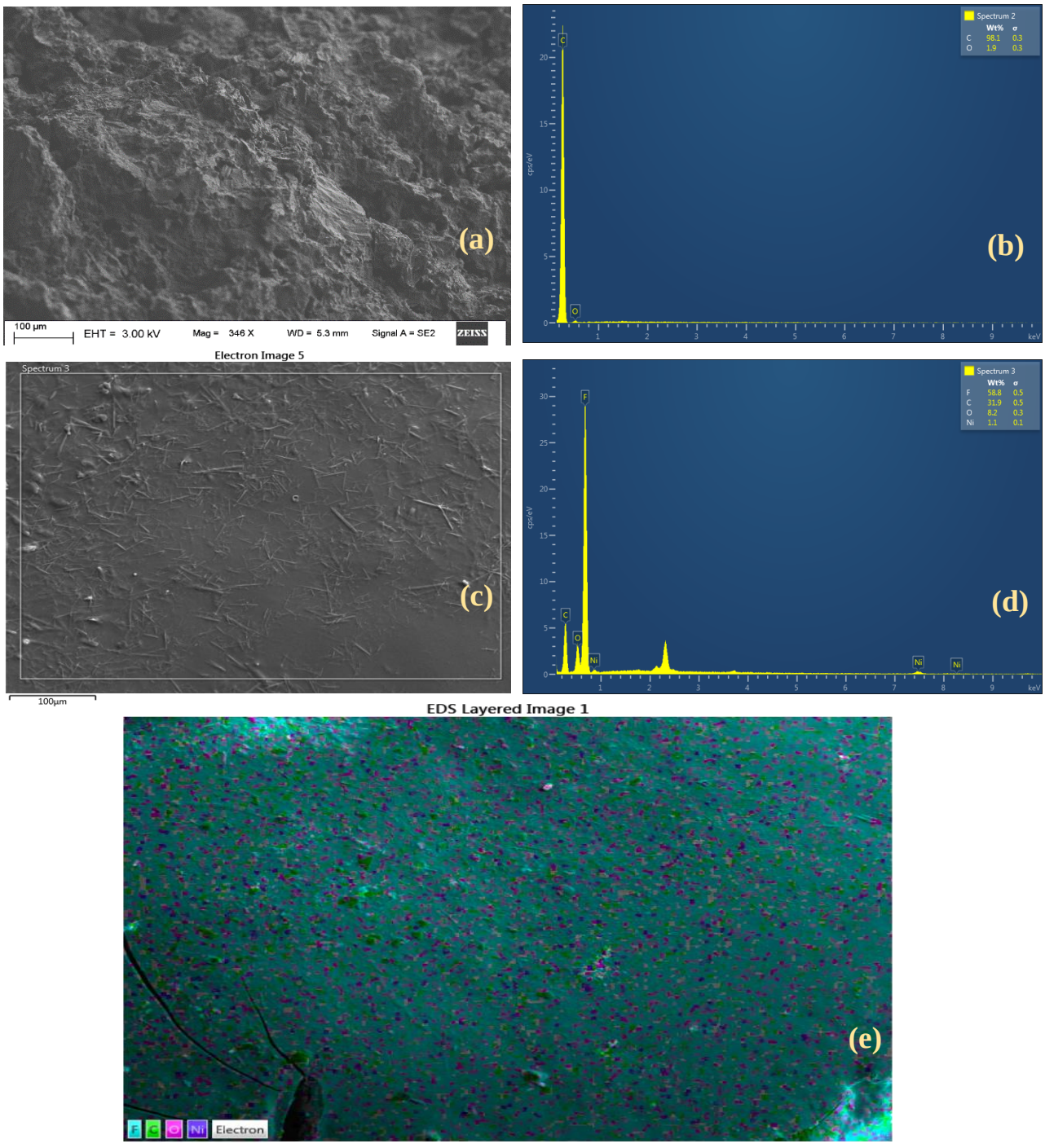

Figure S7: Morphology and EDX analysis of $\mathbf{Ni^{II}L^{NH}_2}$ /graphite WE. (a) FE-SEM micrograph of bare graphite WE surface before catalyst coating, (b) Elemental abundance of the bare graphite WE (Fig. 1a), (c) FE-SEM micrograph of fresh surface of $\mathbf{Ni^{II}L^{NH}_2}$/graphite WE, (d) Elemental abundance of $\mathbf{Ni^{II}L^{NH}_2}$/graphite WE and (e) Elemental distribution of $\mathbf{Ni^{II}L^{NH}_2}$/graphite WE.

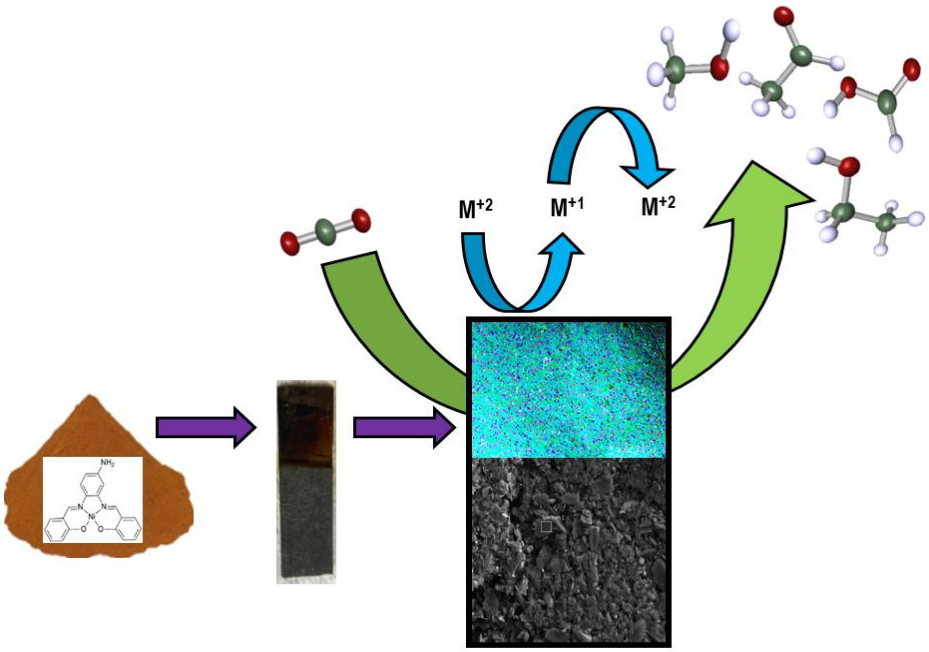

Figure S8: Schematic diagrams of the representation of redox character of the salen metal complex during electrolysis of CO_2.

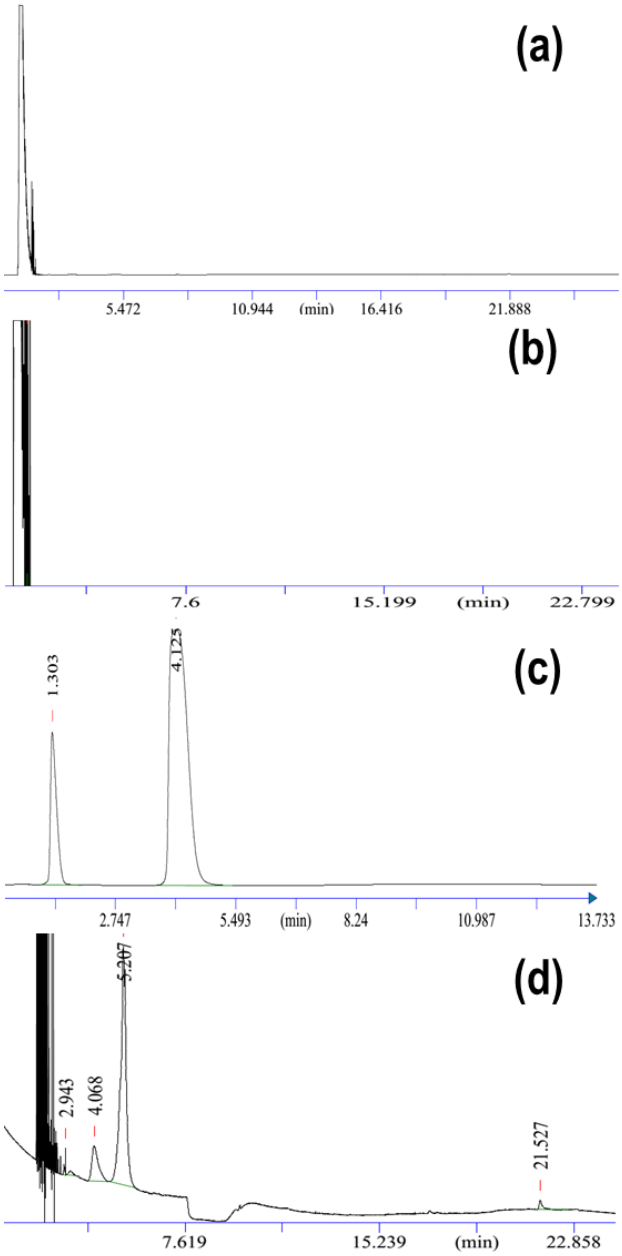

Figure S9: Gas chromatograms showing product formation during ERC using (a) chromatograph of liquid sample only with graphite electrode without the catalyst, (b) chromatograph of liquid sample using $\mathbf{Ni^{II}L^{NH_2}}$/graphite electrode in N_2 atmosphere, (c) chromatograph of gaseous sample using $\mathbf{Ni^{II}L^{NH_2}}$/graphite electrode in N_2 atmosphere, and (d) chromatograph of liquid sample using $\mathbf{Ni^{II}L^{NH_2}}$/graphite electrode with CO_2 atmosphere after 1 h of electrolysis at -1.8 V vs. Ag/AgCl. RT= 2.94 min for CH_3CHO, RT = 4.068 for CH_3OH, RT= 5.2 for C_2H_5OH and RT= 21.5 is for HCOOH using $\mathbf{Ni^{II}L^{NH_2}}$ /graphite WE in Fig. S7b. RT = 1.3 min is for H_2 and RT = 4.125 min is for N_2 in Fig. S7d.

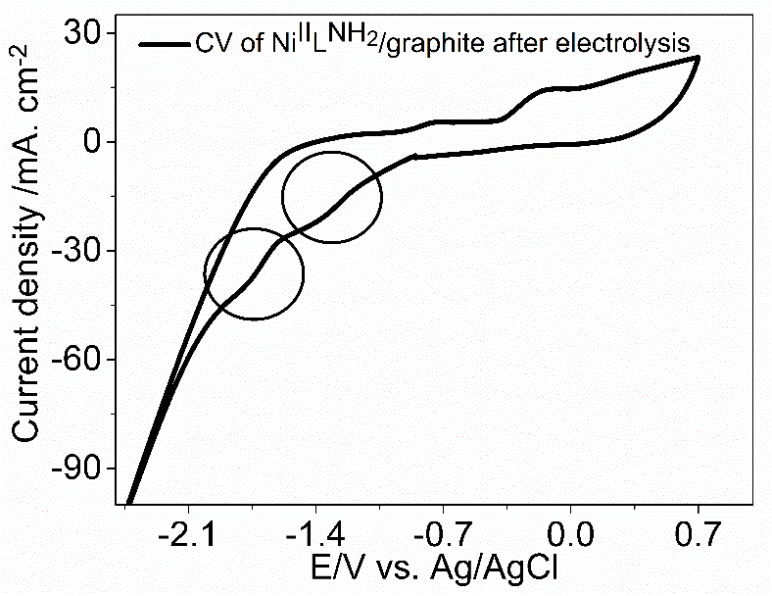

Figure S10: CV curve at a scan rate of 30 mV s^{-1} during ERC at $\mathbf{Ni^{II}L^{NH}_2}$ /graphite WEs CO_2 saturation after 1 hour of electrolysis. Experimental condition: Electrolyte 0.5 mM $KHCO_3$, catholyte and anolyte 120 mL each and ~45 min initial pre-saturation time.

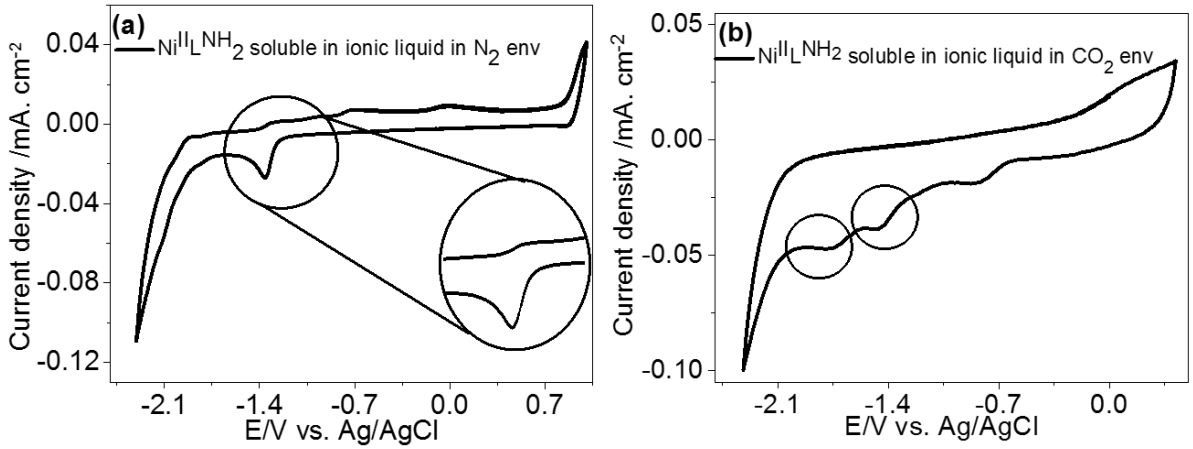

Figure S11: CV curves at a scan rate of 100 mV s^{-1} at glassy carbon WE in1 mM $\mathbf{Ni^{II}L^{NH}_2}$ complex as analyte at (a) N_2 saturation and (b) CO_2 saturation. Experimental condition: Electrolyte 0.1 M $TBAPF_6$ in CH_3CN solution, Pt wire as CE and Ag/AgCl as RE.

References

1 M. Azuma, K. Hashimoto and M. Hiramoto, J. Electrochem. Soc, 1990, **137**, 1772-1778.

2 Y. Liu, S. Chen, X. Quan and H. Yu, J. Am. Chem. Soc, 2015, **137**, 11631–11636.

3 E. R. Cave, J. H. Montoya, K. P. Kuhl, D. N. Abram, T. Hatsukade, C. Shi, C. Hahn, K. Nørskov and T. F. Jaramillo, Phys. Chem. Chem. Phys, 2017, **19**, 15856–15863.

4 L. Cao, H. Huang, J. Wang, D. Zhong and T. Lu, Green Chem, 2018, **20**, 798–803.

5 J. Honores, D. Quezada, M. García, K. Calfumán, J. P. Muena, M. J. Aguirre, M. C. Arévalo and M. Isaacs, *Green Chem.*, 2017, **19**, 1155–1162.

6 L. E. Lieske, A. L. Rheingold and C. W. Machan, Sustain. Energy Fuels, 2018, **2,** 1269–1277.